5-Iodotubercidin inhibits SARS-CoV-2 RNA synthesis

Jianyuan Zhao [a,b,1], Qian Liu [b,1], Dongrong Yi [a], Quanjie Li [a], SaiSai Guo [a], Ling Ma [a], Yongxin Zhang [a], Dongxin Dong [b], Fei Guo [c], Zhenlong Liu [a,d], Tao Wei [b,**], Xiaoyu Li [a,***], Shan Cen [a,*]

[a] *Institute of Medicinal Biotechnology, Chinese Academy of Medical Science, Beijing, China*
[b] *Beijing Key Laboratory of Bioactive Substances and Functional Foods, Beijing Union University, China*
[c] *Institute of Pathogen Biology, Chinese Academy of Medical Science, Beijing, China*
[d] *Lady Davis Institute for Medical Research, Jewish General Hospital, Division of Experimental Medicine, Department of Medicine, McGill University, Montreal, Quebec, Canada*

ARTICLE INFO

ABSTRACT

Coronavirus disease 2019 (COVID-19) is a newly emerged infectious disease caused by a novel coronavirus, the severe acute respiratory syndrome coronavirus 2 (SARS-CoV-2). The rapid global emergence of SARS-CoV-2 highlights the importance and urgency for potential drugs to control the pandemic. The functional importance of RNA-dependent RNA polymerase (RdRp) in the viral life cycle, combined with structural conservation and absence of closely related homologs in humans, makes it an attractive target for designing antiviral drugs. Nucleos(t)ide analogs (NAs) are still the most promising broad-spectrum class of viral RdRp inhibitors. In this study, using our previously developed cell-based SARS-CoV-2 RdRp report system, we screened 134 compounds in the Selleckchemicals NAs library. Four candidate compounds, Fludarabine Phosphate, Fludarabine, 6-Thio-20-Deoxyguanosine (6-Thio-dG), and 5-Iodotubercidin, exhibit remarkable potency in inhibiting SARS-CoV-2 RdRp. Among these four compounds, 5-Iodotubercidin exhibited the strongest inhibition upon SARS-CoV-2 RdRp, and was resistant to viral exoribonuclease activity, thus presenting the best antiviral activity against coronavirus from a different genus. Further study showed that the RdRp inhibitory activity of 5-Iodotubercidin is closely related to its capacity to inhibit adenosine kinase (ADK).

1. Introduction

Coronavirus disease 2019 (COVID-19) is a newly emerged infectious disease caused by a novel coronavirus, the severe acute respiratory syndrome coronavirus 2 (SARS-CoV-2) (Chen et al., 2020a). The disease has been recognized as the most serious global threat in the past decades, as it rapidly spreads worldwide, causing significant health and economic losses in many countries (WHO, 2022). The clinical manifestations of COVID-19 include fever, fatigue, dry cough, and some less common symptoms such as headache, hemoptysis, and diarrhea (Wu and McGoogan, 2020). While most patients develop dyspnea and pneumonia, some severe cases might deteriorate into respiratory failure, septic shock, and/or multiple organ failure, eventually leading to death

(Chen et al., 2020b). The rapid global emergence of SARS-CoV-2 highlights the importance and urgency for potential drugs to control the pandemic.

SARS-CoV-2 is an enveloped, positive-sense, single-stranded RNA virus (Hu et al., 2015; Li et al., 2005). The SARS-CoV-2 genome comprises 29.8 kb and has 14 open reading frames (ORFs), which encode information for 27 structural and non-structural proteins (Hu et al., 2021; V'Kovski et al., 2021). At the 5′-end of the genome, there are two overlapping ORFs (ORF-1a and ORF-1ab) encoding the replicase genes of the virus. The replicase genes are directly translated from the viral genome, while other downstream genes encoding structural and accessory proteins are derived from viral subgenomic mRNAs. ORF-1a and ORF-1ab encode two large replicase polyproteins (PP1a and PP1ab),

---

which are further cleaved by papain-like cysteine protease and 3 chymotrypsin-like cysteine protease to produce 16 nonstructural proteins (nsp1 to nsp16) for viral replication and transcription (Wu et al., 2020; Zhou et al., 2020).

The SARS-CoV-2 nonstructural proteins papain-like protease (nsp3), chymotrypsin-like main protease (3CL protease, nsp5), primase complex (nsp7–nsp8), RNA-dependent RNA polymerase (nsp12), helicase (nsp13) and exoribonuclease (nsp14) are essential for its replication (Hu et al., 2021). While nsp12 serves as the core component of RNA-dependent RNA polymerase (RdRp), which catalyzes the viral genome replication and transcription, its functions require two other factors, nsp7 and nsp8, which stabilize nsp12 regions involved in RNA binding and confers processivity to it (Gao et al., 2020; Tvarogová et al., 2019). Further studies have indicated that the exoribonuclease activity of the nsp14 confers the proofreading function, thus ensuring the replication fidelity of the virus. The functional importance of RdRp in the viral life cycle, combined with structural conservation and the absence of closely related homologs in humans, makes it an attractive target for the design of antiviral drugs (Hillen et al., 2020).

Nucleos(t)ide analogs (NAs) and nonnucleoside inhibitors (NNIs) are two types of RdRp inhibitors. NAs are prodrugs that can be converted into the corresponding active form (triphosphate structure) in host cells and incorporated into the viral RNA chain by RdRp, which can cause a lethal mutation or terminate RNA synthesis. Unlike NAs that directly inhibit the viral polymerase, NNIs change the spatial conformation of RdRp by binding to allosteric sites of the enzyme and thereby inhibit its activity and the synthesis of viral RNA. For NNIs are more susceptible to drug resistance and cannot affect other subtypes, limiting their development, NAs are still the most promising broad-spectrum class of viral RdRp inhibitors. At present, although many NAs have been trialed against SARS-CoV-2 infections (Abdelnabi et al., 2017; Choy et al., 2020; Elfiky, 2020a; Jockusch et al., 2020; Kaptein et al., 2020; Venkateshan et al., 2020), only Remdesivir has been approved by the United States Food and Drug Administration (FDA) and molnupiravir have been approved by the United Kingdom for prevention and treatment of COVID-19.

In this study, we screened the NAs library of Selleckchemicals company for their anti-SARS-CoV-2 activities using our cell-based SARS-CoV-2 RdRp report system, aiming at finding new potential RdRp inhibitors of SARS-CoV-2.

2. Materials and methods

2.1. Cells lines and viruses

HEK293T, HCT-8 and LLC-MK2 cells were cultured in Dulbecco's modified Eagle's medium (DMEM; Gibco, Thermo Fisher Scientific, Waltham, MA, USA) with 10% (v/v) heat-activated fetal bovine serum (FBS; Gibco, Thermo Fisher Scientific, Waltham, MA, USA). All DNA plasmids were transfected using Vigofect (Vigorous) following the manufacturer's instructions. HCT-8 cells were infected HCoV-OC43 (strains VR-1558) at an MOI of 0.1 and LLC-MK2 cells were infected with HCoV-NL63 (strain Amsterdam I) at an MOI of 0.01.

2.2. Plasmids, antibodies, and chemical reagents

The Flag-tagged optimized pCOVID19-nsp12, pCOVID19-nsp7, pCOVID19-nsp8, pCOVID19-nsp10 and pCOVID19-nsp14 was provided by Dr. Guo Fei. The plasmid pCoV-Gluc is initiated by the CMV (cytomegalovirus) promoter. Detailedly, 5′UTR-Gluc-3′UTR was first synthesized (Sangon Biotech), then inserted into the BamHI and NotI sites of pRetroX-tight-Pur vector. When the amounts of Gluc mRNA were transcribed, the UTRs flanked the mRNA can be recognized and amplified by viral RdRp, producing a large number of Gluc expression.

Antibodies against DYKDDDDK (Flag) Tag (8146) was ordered from Cell Signaling Technology, Inc (CST, USA). Anti-β-actin antibody (ab8224) were purchased from Abcam. ADK (H-1) antibody (sc-514588) and HRP-conjugated goat anti-mouse secondary antibody (sc-2031) were obtained from Santa Cruz Co. The si ADK adenosine kinase [*Homo sapiens* (human)] sequence was: GCTGCTGCCAATTGTTATA.

The Nucleos(t)ide analogs library containing 134 structurally diverse small-molecule compounds was purchased from Selleckchemicals company and Remdesivir were obtained from Target Molecule Corp (Target Mol). All compounds were of a purity >95%.

2.3. Real-time RNA isolation and quantitative RT-PCR

HEK293T cells were treated with Remdesivir or test compounds (2 μM or 10 μM) for 24 h, then total RNA was extracted with TRIzol reagent (Life Technologies). cDNA was synthesized using the special primers which targeting the 5′UTR and Gaussia-luciferase gene. The primers are: Gluc(+) primer (5′-TGG ATC TTG CTG GCG AAT GT-3′) or Gluc (−) primer (5′-ACT GTC GTT GAC AGG ACA CG-3') for 1 h at 37 °C. One pair of oligonucleotides were used to specifically target the Gluc plus or minus strand gene, as follows: Gluc forward (5′-CGG GTG TGA CCG AAA GGT AA-3′) and reverse (5′-TGG ATC TTG CTG GCG AAT GT-3′). GAPDH was used for normalize the Gluc mRNA level and the primers are forward (5′-GTC CAC TGG CGT CTT CAC CA-3′) and reverse (5′-GTG GCA GTG ATG GCA TGG AC-3′). The cDNAs were quantified using SsoFast EvaGreen Supermix (Bio-Rad) in an applied system (Thermo Fisher Scientific).

2.4. Cell toxicity assay

The cell toxicity was measured using CCK-8 kit (Beyotime), which is a water-soluble tetrazolium salt-8 (WST-8) reagent. Briefly, HEK293T cells were seeded in 96-well plates with a density of 4×10^4 cells per well one day before compounds were added. Then 1 μL of each tested compound was added to each well and incubated for another 24 h. After incubation, 10 μL of CCk-8 reagent was added into each well and incubated for 60 min at 37 °C with 5% CO_2. The absorbance at 450 nm was measured using the Enspire 2300 Multiable reader (PerkinElmer). The 50% cytotoxic concentration (CC_{50}) was calculated by comparing the viability of test compounds-treated cells with that of DMSO-treated cells.

2.5. Gluc activity assay

Coelenterazine-h (Promega, Madison, WI, USA) was dissolved in absolute ethyl alcohol to a concentration of 1.022 mmol/L. Then, the stock was diluted in PBS to 16.7 μM and incubated in the dark for 30 min at room temperature. For the luminescence assay, the cell supernatant was collected for 10 μL to a white and opaque 96-well plate and mixed with 60 μL of 16.7 μM coelenterazine-h. The luminescence was acquired using the Berthold Centro XS3 LB 960 microplate luminometer (Berthold Technologies, Bad Wildbad, Germany). The EC_{50} values were obtained by non-linear regression analysis using GraphPad Prism 8.0.

2.6. Anti-coronavirus activity assay

The MTS Cell Proliferation Colorimetric assay kits (Promega, Madison, WI, USA) was used for measuring anti-HCoV-OC43 and anti-HCoV-NL63 activities of tested compounds. HCT-8 and LLC-MK2 cells were seeded into 96 wells (2×10^4/well) for 24 h, and then infected with HCoV-OC43 (MOI = 0.1) and HCoV-NL63 (MOI = 0.01), respectively, containing 2% FBS and each of the test compounds. Cells were incubated at 33 °C for 5 days, then 20 μL of MTS Cell Proliferation Colorimetric reagent was added into each well and incubated for 3 h at 37 °C with 5% CO_2. The optical density at 490 nm wavelength was recorded using a Enspire 2300 Multiable reader (PerkinElmer).

The percentage CPE inhibition was follows: The percentage CPE inhibition =(A_{490} of samples−A_{490} of negative control)/(A_{490} of positive

control −A_{490} of negative control) × 100. Notes: Cells with virus infection but without drugs were defined as negative control with 0% CPE inhibition. And cells without virus infection was defined as positive control with 100% CPE inhibition.

2.7. Statistical analysis

Data are presented as the means ± SD from at least three independent experiments, and the two-tailed *t*-test were used for statistical analysis. Statistical differences are indicated as follows: P < 0.05(*), P < 0.01(**) and P < 0.001(***).

3. Result

3.1. Screening of anti-SARS-CoV-2 RdRp compounds

Previously, we have reported a cell-based SARS-CoV-2 RdRp activity assay system that can be deployed to screen SARS-CoV-2 RdRp inhibitors (Zhao et al., 2021). The system is composed of a Gaussia-luciferase (Gluc) reporter plasmid and the plasmids for expressing SARS-CoV-2 RdRp, composed of nsp12, nsp7, and nsp8. The Gluc gene, flanked untranslated regions (UTRs) of SARS-CoV-2 in its 5′ and 3′ terminals, was under a tetracycline-regulated expression promoter. When trace amounts of Gluc mRNA were transcribed, the UTRs flanked the mRNA can be recognized and amplified by viral RdRp, resulting in the substantial increase of Gluc expression (Fig. 1A). Therefore, the Gluc activity presents the activity of SARS-CoV-2 RdRp. Using this assay, we evaluated the inhibitory activity of the compounds against SARS-CoV-2 RdRp in the Selleckchemicals NAs library. Of the 134 compounds tested, 4 compounds Fludarabine Phosphate, Fludarabine, 6-Thio-dG, and 5-Iodotubercidin, showed potent activity at 10 µM, whose inhibition ratio was 89.78%, 88.71%, 75.19% and 85.69%, respectively (Fig. 1B).

3.2. Inhibitory activity of fludarabine phosphate, fludarabine, 6-thio-dG, and 5-iodotubercidin upon SARS-CoV-2 RdRp

Using Remdesivir as a positive control, we measured the four compounds' 50% effect concentration (EC$_{50}$) value. The compounds Fludarabine Phosphate, Fludarabine, 6-Thio-dG, and 5-Iodotubercidin, displayed remarkable potency in inhibiting SARS-CoV-2 RdRp with EC$_{50}$ values of 0.93 µM, 1.06 µM and 1.08 µM and 0.75 µM respectively, close to that of Remdesivir (1.07 µM). We further determined the in vitro 50% cytotoxic concentration (CC$_{50}$) for defining therapeutic index (TI) (CC$_{50}$/EC$_{50}$). Among the four compounds, 5-Iodotubercidin showed the best SARS-CoV-2 RdRp inhibitory activity, which was even better than the Remdesivir (Fig. 2 A-E upper panel and Table 1). The CC$_{50}$ values of the four compounds were 65.24 µM, 53.62 µM, more than 100 µM and 59.46 µM respectively (Fig. 2 A-E lower panel and Table 1), with the TI

value of 70.15, 50.58, over 92.59 and 79.28, respectively. These compounds showed strong inhibiting activity against SARS-CoV-2 RdRp and relatively low cytotoxicity (see Fig. 2).

3.3. Fludarabine phosphate, fludarabine, 6-thio-dG, and 5-iodotubercidin inhibit SARS-CoV-2 RNA synthesis

To further confirm whether these compounds can inhibit the SARS-CoV-2 RdRp for the synthesis of viral RNA, we examined the effect of these compounds on viral RNA synthesis by quantifying the plus-strand and minus-strand RNA levels Gluc. The results indicated that all these four compounds and Remdesivir could diminish the levels of both plus-strand RNA and minus-strand Gluc RNA in a dose-dependent manner. Among the four compounds tested, the inhibitory activity of 5-Iodotubercidin was even better than the Remdesivir (Fig. 3). The results were consistent with the previous in-cell Gluc report system result, further confirming that Fludarabine Phosphate, Fludarabine, 6-Thio-dG, and 5-Iodotubercidin are potent SARS-CoV-2 RdRp inhibitors(Yin et al., 2020).

3.4. Fludarabine phosphate, fludarabine, 6-thio-dG, and 5-iodotubercidin were resistant to proofreading activity of nsp14/nsp10

One major challenge in designing NA drugs is that NAs incorporated into RNA can be removed by the CoV proofreading function, limiting NAs potency. During coronavirus replication, exoribonuclease nsp14 and its activator nsp10 excise erroneous mutagenic nucleotides incorporated by nsp12 into viral RNA, thus producing resistance to NA drugs (Ma et al., 2015). Many NAs such as Ribavirin can be excised from the growing RNA chain of CoVs, thus immensely reducing its antiviral activity (Ferron et al., 2018). Therefore, its necessary to explore whether the inhibition activity of four screened NA compounds were affected by the presence of nsp14 and nsp10.

In this study, we expressed nsp14 and nsp10 in the cell-based CoV-RdRp-Gluc system. Compared to Ribavirin which was sensitive to proofreading activity of viral nsp14 and nsp10, with the EC$_{50}$ value of more than 1000 µM (Fig. 4F), Fludarabine Phosphate, Fludarabine and 6-Thio-dG also increased their EC$_{50}$ values against SARS-CoV-2 RdRp in the presence of nsp14 and nsp10, with the EC$_{50}$ values of 6.69 µM, 12.22 µM and 8.68 µM respectively (Fig. 4 and Table 2). Moreover, 5-Iodotubercidin exhibited the most potent proofreading-resistant activity, even better than that of Remdesivir (Fig. 4D). These results demonstrate that among these four compounds, only 5-Iodotubercidin was insensitive to exoribonuclease activity of SARS-CoV-2 RdRp, which would be a great advantage over other NAs.
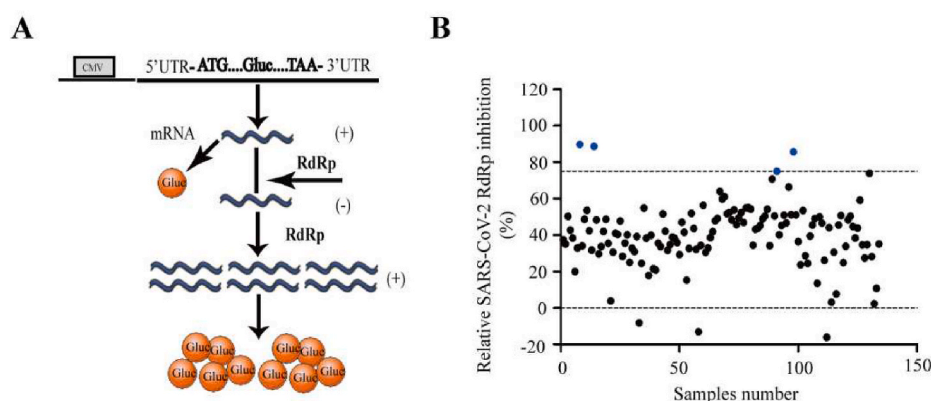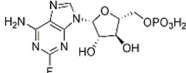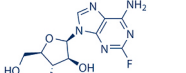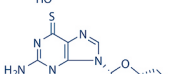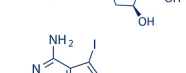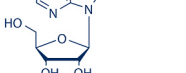

Fig. 1. Screening for anti-SARS-CoV-2 RdRp compounds. (A) The sketch map of the Gluc reporter system. The expression cassette of Gluc is in the sense strand, which is flanked by the 5′ and 3′ untranslated regions (UTRs) of SARS-CoV-2. The negative-sense vRNA is first synthesized by SARS-CoV-2 RdRp (nsp12, nsp7, and nsp8), followed by transcription into plus-strand RNA (mRNA) to magnify the Gluc signal. (B) The screen result of the 134 NAs compounds for the inhibition activity against SARS-CoV-2 RdRp. The blue spots represent compounds Fludarabine Phosphate, Fludarabine, 6-Thio-dG, and 5-Iodotubercidin, which inhibitory activity >75%.
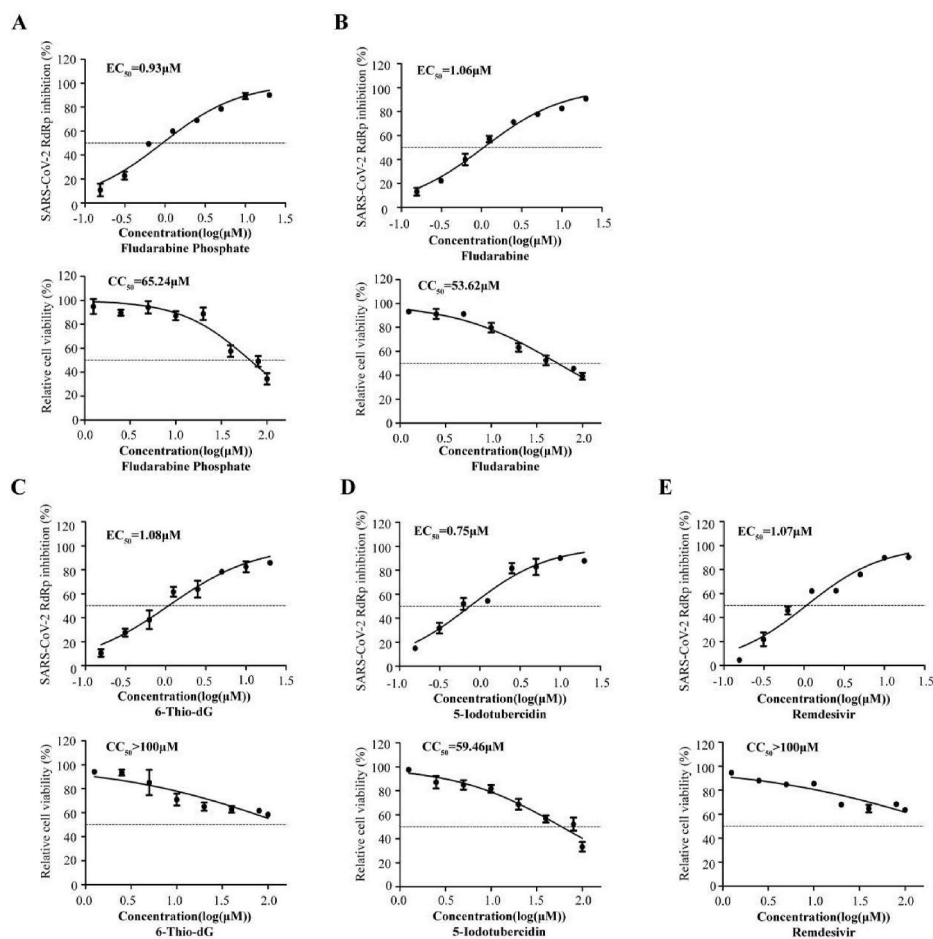
Fig. 2. Dose-response curves (EC$_{50}$ and CC$_{50}$) for the top 4 compounds. HEK293T cells were transfected with CoV-Gluc, nsp12, nsp7, and nsp8 plasmid at the ratio of 1:10:30:30. Twelve hours post-transfection, cells were re-seeded in 96-well plates (104/well) and then treated with two-fold serially diluted Fludarabine Phosphate, Fludarabine, 6-Thio-dG, 5-Iodotubercidin, and Remdesivir (from 0.16 to 20 μM). After 24 h of incubation, Gluc activity in supernatants was determined. EC50 value was shown in (A-E upper panel). HEK293T cells (104/wells) were seeded in 96-well plates and treated with two-fold serially diluted these inhibitors (from 1.25 to 100 μM), as indicated above, to assess cell viability. The CC50 values were measured with CCK-8 Kit as also shown in (A-E lower panel). Data represent the mean ± standard deviation (error bars) of the results of three independent experiments.

Table 1
Structure, properties, and antiviral activities of 4 compounds against SARS-CoV-2 RdRp.

| Structure	Compound name	Cas no.	Formula	RdRp EC$_{50}$ (μM)	CC$_{50}$ (μM)	TI (CC$_{50}$/EC$_{50}$)
	Fludarabine Phosphate	75607-67-9	$C_{10}H_{13}FN_5O_7P$	0.93	65.24	70.15
	Fludarabine	21679-14-1	$C_{10}H_{12}FN_5O_4$	1.06	53.62	50.58
	6-Thio-dG	789-61-7	$C_{10}H_{13}N_5O_3S$	1.08	>100	>92.59
	5-Iodotubercidin	24386-93-4	$C_{11}H_{13}IN_4O_4$	0.75	59.46	79.28
	Remdesivir			1.07	>100	>93.46

3.5. SARS-CoV-2 RdRp inhibitory activity of 5-iodotubercidin was related to its ADK inhibitory activity

For 5-iodotubercidin has the most potent inhibitory activity against SARS-CoV-2 RdRp among the four candidates NA compounds, we next focused on the mechanisms of its inhibitory activity. We first hypothesized that active form 5-iodotubercidin might be incorporated into the viral RNA chain by interaction with SARS-CoV-2 RdRp like other NAs.

Surprisingly, we did not detect the binding activity of 5-iodotubercidin upon SARS-CoV-2 RdRp using Bio layer interferometry assay, which has been widely used to detect biomolecular interactions in real-time (data not shown).

However, we noticed that 5-iodotubercidin was previously characterized as an adenosine kinase (ADK) inhibitor and has been widely used to study the effects of adenosine (Davies et al., 1986). We thus speculated that this inhibitor activity might be related to its RdRp restricting

Fig. 3. Inhibition of CoV-Gluc RNA expression by Fludarabine Phosphate, Fludarabine, 6-Thio-dG, and 5-Iodotubercidin. HEK293T cells were transfected with CoV-Gluc, nsp12, nsp7, nsp8 plasmid DNA at the ratio of 1:10:30:30. Six hours post-transfection, supernatants were replaced with fresh medium containing Fludarabine Phosphate(A), Fludarabine(B), 6-Thio-dG(C), 5-Iodotubercidin(D), and Remdesivir(E), respectively. Cells were cultured for another 24 h, and total cellular RNA was extracted. CoV-Gluc RNA was determined by real-time qRT-PCR. Data represent the mean ± standard deviation (error bars) of the results of three independent experiments. **P < 0.01, ***P < 0.001.
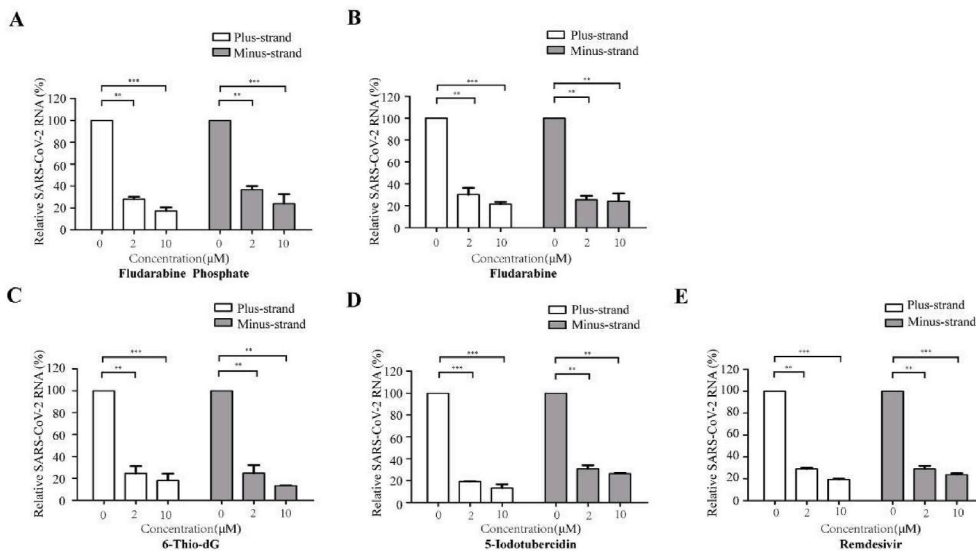
Fig. 4. 5-Iodotubercidin was resistant to proofreading activity of nsp14/nsp10. HEK293T cells were co-transfected CoV-Gluc, nsp12, nsp7, nsp8 with or without nsp10, and nsp14 plasmid at the ratio of 1:10:30:30:25:25. Using Remdesivir and Ribavirin as positive and negative control respectively (E and F), the EC_{50} value of Fludarabine Phosphate(A), Fludarabine(B), 6-Thio-dG(C), and 5-Iodotubercidin(D) was determined respectively by the cell-based system with nsp10/nsp14 proofreading function.The active compounds was two-fold serially diluted (from 1.25 to 100 μM). Data represent the mean ± standard deviation (error bars) of the results of three independent experiments.
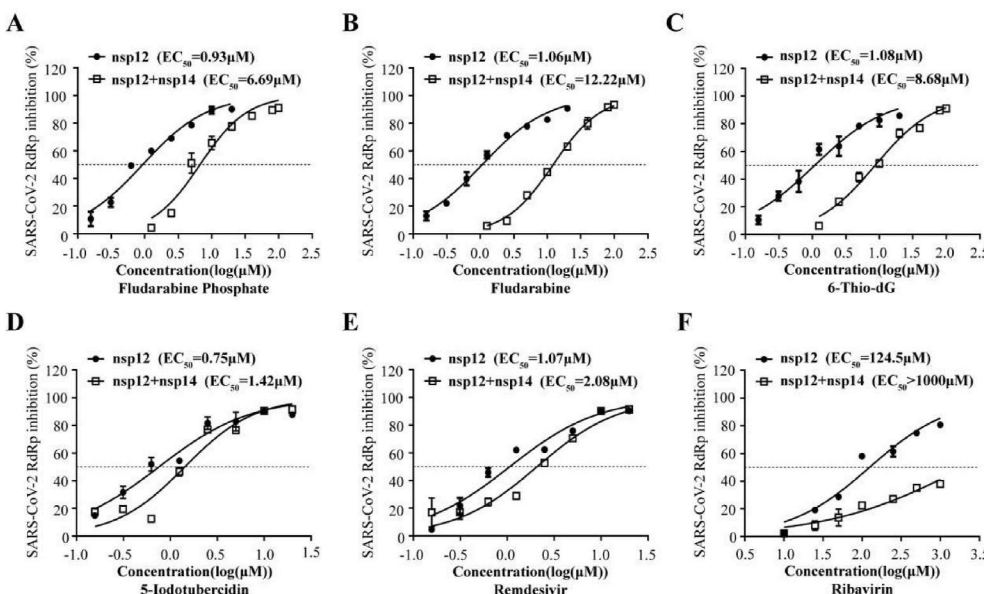
Table 2
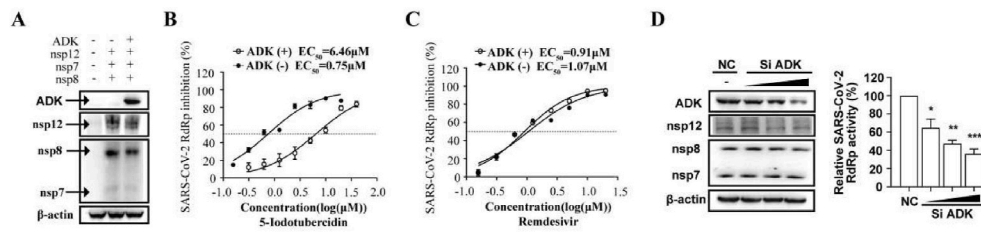Summary of positive compounds on inhibition of SARS-CoV-2 RdRp.

Compounds	Nsp12 (EC_{50}/μM)	Nsp12 + 14 (EC_{50}/μM)	Ratio (12 + 14/12)
Fludarabine Phosphate	0.93	6.69	7.19
Fludarabine	1.06	12.22	11.53
6-Thio-dG	1.08	8.68	8.04
5-Iodotubercidin	0.75	1.42	1.89
Remdesivir	1.07	2.08	1.94
Ribavirin	124.5	>1000	>8.03

activity. To test this, we first measured the EC_{50} value of 5-iodotubercidin against SARS-CoV-2 RdRp in the presence of ADK and found that the over-expression of ADK significantly compromised the SARS-CoV-2 RdRp inhibitory activity (Fig. 5A and B), and by contrast, the ADK over-expression has no obvious effect upon the inhibitory activity of Remdesivir (Fig. 5C). Furthermore, we also found that when endogenous ADK was knocked down with increasing amounts of short

interfering RNA (siRNA), the SARS-CoV-2 RdRp was also decreased in a dose-dependent manner (Fig. 5D). These results suggested that the ADK inhibitor activity of 5-iodotubercidin was closely related to its SARS-CoV-2 RdRp inhibitory activity.
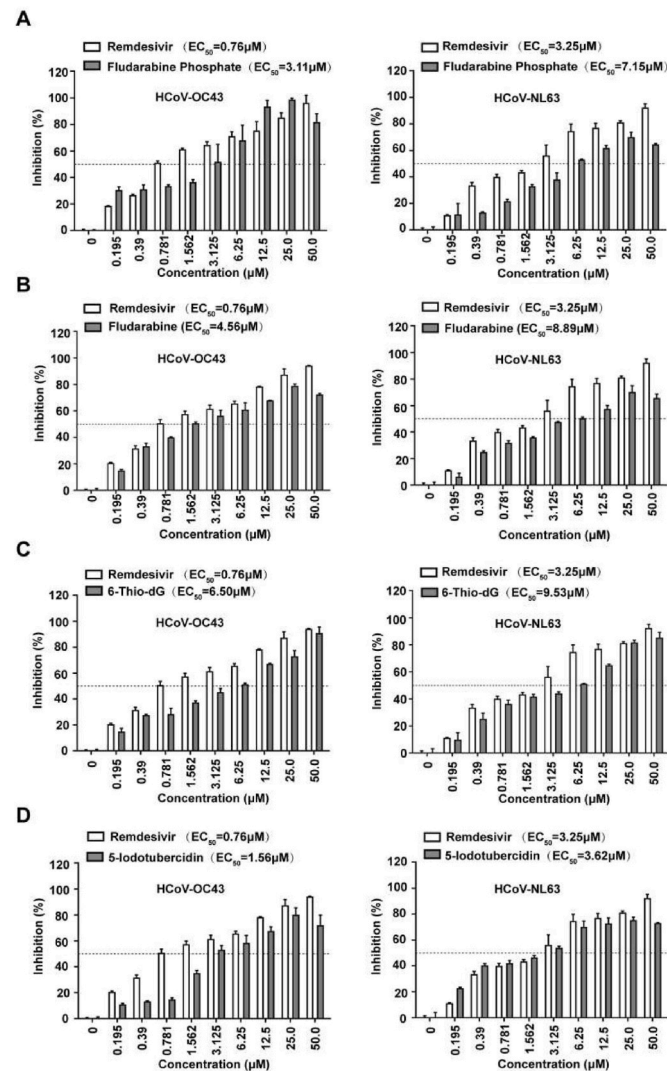
3.6. Evaluation of the antiviral activity of fludarabine phosphate, fludarabine, 6-thio-dG, and 5-iodotubercidin against human coronavirus strain HCoV-OC43 and HCoV-NL63

To assess if these compounds were effective against the replication of coronavirus, a cell-based assay was utilized using HCT-8 and LLC-MK2 cell line infected with coronavirus strains HCoV-OC43 and HCoV-NL63, which belong to beta coronaviruses and alphacoronaviruses, respectively, followed by measuring the protection of cell viability against CoV-induced cytopathic effect (CPE) as a read-out (Li et al., 2021). Using Remdesivir as a positive control, we infected HCT-8 or LLC-MK2 cells with these two coronavirus strains at MOI of 0.1 and 0.01 respectively and then treated the cells with serial dilutions of the four compounds. As shown in Fig. 6, Fludarabine Phosphate, Fludarabine,

Fig. 6. Evaluation of the antiviral activity of 5-Iodotubercidin against human coronavirus strain HCoV-OC43 and HCoV-NL63. HCT-8 and LLC-MK2 were infected by HCoV-OC43 (A) or HCoV-NL63 (B) at an MOI of 0.1 and 0.01, respectively, and treated with two-fold serially diluted (from 0.195 to 50 μM) to evaluate the antiviral activity of Fludarabine Phosphate, Fludarabine, 6-Thio-dG, 5-Iodotubercidin, and Remdesivir 1 h post-infection. The impact of treatment on cell viability was measured by MTS assay after 5 days post-infection. Data represent the mean ± standard deviation (error bars) of the results of three independent experiments.

6-Thio-dG, and 5-Iodotubercidin exhibited a dose-dependent inhibitory effect on the replication of both viruses with the EC$_{50}$ value of 3.11 μM, 4.56 μM, 6.50 μM, 1.56 μM respectively in HCoV-OC43 and 7.15 μM, 8.89 μM, 9.53 μM, 3.62 μM respectively in HCoV-NL63. Further more, we also measured the CC$_{50}$ values of the four active compounds after incubation for 5 days in HCT-8 and LLC-MK2 cells. Results shown that their CC$_{50}$ values were rang from 37.47 to 63.02 μM and 45.58–67.99 μM in HCT-8 and LLC-MK2 cells respectively (Table 3). Overall their CC$_{50}$ values are much larger than their EC$_{50}$ values of the cytopathic effects (CPE) assay both in HCT-8 and LLC-MK2 Cells (Fig. 6). The results showed these compounds were effective upon HCoV-OC43 and HCoV-NL63, but more sensitive to HCoV-OC43 which also belonged to the betacoronavirus genus.

4. Discussion

The rapid global emergence of SARS-CoV-2 highlights the urgency for potential drugs to control the pandemic. The RdRp presents an optimal target due to its crucial role in RNA viruses, including SARS-CoV-2. Many compounds such as ribavirin, favipiravir, and penciclovir were shown to have inhibitory effects on activity towards SARS-CoV-2 RdRp in vitro or computer-aided molecular modeling studies (Elfiky, 2020b; Faheem et al., 2020). In this study, using our previously developed cell-based SARS-CoV-2 RdRp report system, we screened 134 compounds in the Selleckchemicals NAs library for antiviral compounds which can inhibit SARS-CoV-2 RdRp. Four compounds Fludarabine Phosphate, Fludarabine, 6-Thio-dG, and 5-Iodotubercidin showed excellent SARS-CoV-2 RdRp inhibitory and antiviral activity. Fludarabine Phosphate, Fludarabine, and 6-Thio-dG are typical NA prodrugs that can be incorporated into DNA during the nucleic acid chain synthesis for different kinds of cancer therapy (Avramis and Plunkett, 1982; Huang et al., 1990; Sugarman et al., 2019). 5-Iodotubercidin was initially used as an adenosine kinase inhibitor which inhibits the phosphorylation of adenosine to AMP within the cells. In recent years, 5-Iodotubercidin was also revealed to target other kinases, including Cdc2-like kinases (CLKs), dual-specificity tyrosine (Y)-phosphorylation-regulated kinases (DYRKs), and haspin (De Antoni et al., 2012; Massillon et al., 1994; Ugarkar et al., 2000).

Like other RNA viruses, SARS-CoV-2 continually emerges new variants. Among large numbers of detected SARS-CoV-2 variants, some of them can threaten public health, as they are more contagious, cause more severe conditions, and impact vaccine effectiveness. RdRp is

Table 3
Toxicity of the four active compounds.

Compounds	Toxicity CC$_{50}$/μM	
	HCT-8	LLC-MK2
Fludarabine Phosphate	37.47 ± 1.62	60.63 ± 8.93
Fludarabine	40.36 ± 8.16	54.12 ± 7.37
6-Thio-dG	63.02 ± 3.52	67.99 ± 7.03
5-Iodotubercidin	46.93 ± 2.37	45.58 ± 5.15

structurally conserved within RNA viruses including SARS-CoV-2, Fludarabine Phosphate, Fludarabine, 6-Thio-dG, and 5-Iodotubercidin could be effective upon HCoV-OC43 and HCoV-NL63, which belong to different genera of coronavirus, suggesting that these RdRp inhibitors may have the potential to cover more mutants.

However, using NAs as anti-SARS-CoV-2 drugs is needed to consider their sensibility to exonuclease nsp14 activity, which can excise erroneous mutagenic nucleotides incorporated by nsp12 into viral RNA, thus creating resistance to many NAs. Although Fludarabine Phosphate, Fludarabine, 6-Thio-dG exhibit remarkable potency in inhibiting SARS-CoV-2 RdRp, they are still sensitive to viral infection exoribonuclease activity. Only 5-Iodotubercidin exhibited potent resistance to viral exoribonuclease activity. Unlike most NA inhibitors with similar structures to nucleotides to be incorporated into growing viral RNA strands or act as chain terminators to stop the viral RNA synthesis, 5-Iodotubercidin did not bind to RdRp of the SARS-CoV-2. Although we did not know whether the ADK inhibitory activity is sufficient to confer total antiviral activity of the 5-Iodotubercidin, the evidence of our study points to the importance of its ADK inhibitory activity. It has been reported that 5-Iodotubercidin can interfere with adenosine metabolism and decrease the concentration of ATP in host cells (Flückiger-Isler and Walter, 1993). It is plausible that the depletion of ATP may impair the viral RNA synthesis, thus inhibiting the viral replication.

Although fludarabine, fludarabine phosphate, and 6-thio-dG are known DNA polymerase inhibitors and normally their inhibitory activity for RNA polymerase are low, it has been reported fludarabine exhibited broad antiviral activity against emerging RNA viruses, including ZIKV, EV-A71 and SFTSV (Severe fever with thrombocytopenia syndrome virus). Especially, fludarabine was proposed to impair viral RNA replication (Gao et al., 2021). Furthermore, trimethyl derivatives of fludarabine have shown strong anti-DENV activity (McGuigan et al., 2016). In addition, our data herein revealed that fludarabine, fludarabine phosphate, and 6-thio-dG were sensitive to nsp10/14, which is responsible for removing incorporated nucleoside analog from the synthesized viral RNA chain, providing indirectly evidence supporting their activity against viral RNA synthesis.

On the other hand, we noticed that 5-Iodotubercidin has much better nsp14 resistance activity than the other three NA compounds, which is probably because that the antiviral activity of the 5-Iodotubercidin is related to the ADK inhibitory activity instead of acting directly on viral RdRp, which allows 5-Iodotubercidin to circumvent the exoribonuclease activity of the nsp14. In a word, the exact molecular mechanism of 5-Iodotubercidin is still worth studying. Optimization to reduce the cytotoxicity and increase the cellular activity is also necessary to develop a series of compounds as broad-spectrum anti-coronavirus drugs in the future. Of note, these compounds will likely face a challenging regulatory path for approval given their anti-cancer indications, however, this work clearly validates the utility of this assay and provides a path towards understanding the mechanism of action about antiviral drug or viral RNA synthesis.

Author contribution

SC, TW and XL conceived the idea of project. JZ and QL performed the experiments. DY, QL, SG and DD helped with the resources. LM and YZ contributed to validation. XL drafted the manuscript. FG, ZL and SC reviewed and edited the manuscript. All the authors have read and approved the manuscript for submission.

Declaration of interest statement

We declare that there is no conflict of interest regarding this submission.

Notes

The authors declare no competing financial interest.

References

Abdelnabi, R., Morais, A.T.S., Leyssen, P., Imbert, I., Beaucourt, S., Blanc, H., Froeyen, M., Vignuzzi, M., Canard, B., Neyts, J., et al., 2017. Understanding the mechanism of the broad-spectrum antiviral activity of favipiravir (T-705): Key role of the F1 motif of the viral polymerase. J. Virol. 91.

Avramis, V.I., Plunkett, W., 1982. Metabolism and therapeutic efficacy of 9-beta-D-arabinofuranosyl-2-fluoroadenine against murine leukemia P388. Cancer Res. 42, 2587–2591.

Chen, N., Zhou, M., Dong, X., Qu, J., Gong, F., Han, Y., Qiu, Y., Wang, J., Liu, Y., Wei, Y., et al., 2020a. Epidemiological and clinical characteristics of 99 cases of 2019 novel coronavirus pneumonia in Wuhan, China: a descriptive study. Lancet 395, 507–513.

Chen, T., Wu, D., Chen, H., Yan, W., Yang, D., Chen, G., Ma, K., Xu, D., Yu, H., Wang, H., et al., 2020b. Clinical characteristics of 113 deceased patients with coronavirus disease 2019: retrospective study. Br. Med. J. 368, m1091.

Choy, K.T., Wong, A.Y., Kaewpreedee, P., Sia, S.F., Chen, D., Hui, K.P.Y., Chu, D.K.W., Chan, M.C.W., Cheung, P.P., Huang, X., et al., 2020. Remdesivir, lopinavir, emetine, and homoharringtonine inhibit SARS-CoV-2 replication in vitro. Antivir. Res. 178, 104786.

Davies, L.P., Baird-Lambert, J., Marwood, J.F., 1986. Studies on several pyrrolo[2,3-d] pyrimidine analogues of adenosine which lack significant agonist activity at A1 and A2 receptors but have potent pharmacological activity in vivo. Biochem. Pharmacol. 35, 3021–3029.

De Antoni, A., Maffini, S., Knapp, S., Musacchio, A., Santaguida, S., 2012. A small-molecule inhibitor of Haspin alters the kinetochore functions of Aurora B. J. Cell Biol. 199, 269–284.

Elfiky, A.A., 2020a. Corrigendum to "ribavirin, remdesivir, Sofosbuvir, Galidesivir, and Tenofovir against SARSCoV-2 RNA dependent RNA polymerase (RdRp): a molecular docking study. Life Sci. 253 (2020), 117592. Life sciences 258, 118350.

Elfiky, A.A., 2020b. Ribavirin, remdesivir, Sofosbuvir, Galidesivir, and Tenofovir against SARS-CoV-2 RNA dependent RNA polymerase (RdRp): a molecular docking study. Life Sci. 253, 117592.

Faheem, Kumar B.K., Sekhar, K., Kunjiappan, S., Jamalis, J., Balaña-Fouce, R., Tekwani, B.L., Sankaranarayanan, M., 2020. Druggable targets of SARS-CoV-2 and treatment opportunities for COVID-19. Bioorg. Chem. 104, 104269.

Ferron, F., Subissi, L., Silveira De Morais, A.T., Le, N.T.T., Sevajol, M., Gluais, L., Decroly, E., Vonrhein, C., Bricogne, G., Canard, B., et al., 2018. Structural and molecular basis of mismatch correction and ribavirin excision from coronavirus RNA. Proc. Natl. Acad. Sci. U.S.A. 115, E162–e171.

Flückiger-Isler, R.E., Walter, P., 1993. Stimulation of rat liver glycogen synthesis by the adenosine kinase inhibitor 5-iodotubercidin. Biochem. J. 292 (Pt 1), 85–91.

Gao, C., Wen, C., Li, Z., Lin, S., Gao, S., Ding, H., Zou, P., Xing, Z., Yu, Y., 2021. Fludarabine inhibits infection of Zika virus. SFTS Phlebovirus Enterovirus A71. Viruses 13.

Gao, Y., Yan, L., Huang, Y., Liu, F., Zhao, Y., Cao, L., Wang, T., Sun, Q., Ming, Z., Zhang, L., et al., 2020. Structure of the RNA-dependent RNA polymerase from COVID-19 virus. Science (New York, N.Y.) 368, 779–782.

Hillen, H.S., Kokic, G., Farnung, L., Dienemann, C., Tegunov, D., Cramer, P., 2020. Structure of replicating SARS-CoV-2 polymerase. Nature 584, 154–156.

Hu, B., Ge, X., Wang, L.F., Shi, Z., 2015. Bat origin of human coronaviruses. Virol. J. 12, 221.

Hu, B., Guo, H., Zhou, P., Shi, Z.L., 2021. Characteristics of SARS-CoV-2 and COVID-19. Nat. Rev. Microbiol. 19, 141–154.

Huang, P., Chubb, S., Plunkett, W., 1990. Termination of DNA synthesis by 9-beta-D-arabinofuranosyl-2-fluoroadenine. A mechanism for cytotoxicity. J. Biol. Chem. 265, 16617–16625.

Jockusch, S., Tao, C., Li, X., Chien, M., Kumar, S., Morozova, I., Kalachikov, S., Russo, J. J., Ju, J., 2020. Sofosbuvir terminated RNA is more resistant to SARS-CoV-2 proofreader than RNA terminated by Remdesivir. Sci. Rep. 10, 16577.

Kaptein, S.J.F., Jacobs, S., Langendries, L., Seldeslachts, L., Ter Horst, S., Liesenborghs, L., Hens, B., Vergote, V., Heylen, E., Barthelemy, K., et al., 2020. Favipiravir at high doses has potent antiviral activity in SARS-CoV-2-infected hamsters, whereas hydroxychloroquine lacks activity. Proc. Natl. Acad. Sci. U.S.A. 117, 26955–26965.

Li, Q., Yi, D., Lei, X., Zhao, J., Zhang, Y., Cui, X., Xiao, X., Jiao, T., Dong, X., Zhao, X., et al., 2021. Corilagin inhibits SARS-CoV-2 replication by targeting viral RNA-dependent RNA polymerase. Acta Pharm. Sin. B 11, 1555–1567.

Li, W., Shi, Z., Yu, M., Ren, W., Smith, C., Epstein, J.H., Wang, H., Crameri, G., Hu, Z., Zhang, H., et al., 2005. Bats are natural reservoirs of SARS-like coronaviruses. Science (New York, N.Y.) 310, 676–679.

Ma, Y., Wu, L., Shaw, N., Gao, Y., Wang, J., Sun, Y., Lou, Z., Yan, L., Zhang, R., Rao, Z., 2015. Structural basis and functional analysis of the SARS coronavirus nsp14-nsp10 complex. Proc. Natl. Acad. Sci. U.S.A. 112, 9436–9441.

Massillon, D., Stalmans, W., van de Werve, G., Bollen, M., 1994. Identification of the glycogenic compound 5-iodotubercidin as a general protein kinase inhibitor. Biochem. J. 299 (Pt 1), 123–128.

McGuigan, C., Serpi, M., Slusarczyk, M., Ferrari, V., Pertusati, F., Meneghesso, S., Derudas, M., Farleigh, L., Zanetta, P., Bugert, J., 2016. Anti-flavivirus activity of different tritylated pyrimidine and purine nucleoside analogues. ChemistryOpen 5, 227–235.

Sugarman, E.T., Zhang, G., Shay, J.W., 2019. In perspective: an update on telomere targeting in cancer. Mol. Carcinog. 58, 1581–1588.

Tvarogová, J., Madhugiri, R., Bylapudi, G., Ferguson, L.J., Karl, N., Ziebuhr, J., 2019. Identification and characterization of a human coronavirus 229E nonstructural protein 8-associated RNA 3'-terminal adenylyltransferase activity. J. Virol. 93.

Ugarkar, B.G., DaRe, J.M., Kopcho, J.J., Browne 3rd, C.E., Schanzer, J.M., Wiesner, J.B., Erion, M.D., 2000. Adenosine kinase inhibitors. 1. Synthesis, enzyme inhibition, and antiseizure activity of 5-iodotubercidin analogues. J. Med. Chem. 43, 2883–2893.

V'Kovski, P., Kratzel, A., Steiner, S., Stalder, H., Thiel, V., 2021. Coronavirus biology and replication: implications for SARS-CoV-2. Nat. Rev. Microbiol. 19, 155–170.

Venkateshan, M., Muthu, M., Suresh, J., Ranjith Kumar, R., 2020. Azafluorene derivatives as inhibitors of SARS CoV-2 RdRp: synthesis, physicochemical, quantum chemical, modeling and molecular docking analysis. J. Mol. Struct. 1220, 128741.

WHO, 2022. Coronavirus Disease 2019 (COVID-19) Situation Report.

Wu, F., Zhao, S., Yu, B., Chen, Y.M., Wang, W., Song, Z.G., Hu, Y., Tao, Z.W., Tian, J.H., Pei, Y.Y., et al., 2020. A new coronavirus associated with human respiratory disease in China. Nature 579, 265–269.

Wu, Z., McGoogan, J.M., 2020. Characteristics of and important lessons from the coronavirus disease 2019 (COVID-19) outbreak in China: summary of a report of 72 314 cases from the Chinese center for disease control and prevention. JAMA 323, 1239–1242.

Yin, W., Mao, C., Luan, X., Shen, D.D., Shen, Q., Su, H., Wang, X., Zhou, F., Zhao, W., Gao, M., et al., 2020. Structural basis for inhibition of the RNA-dependent RNA polymerase from SARS-CoV-2 by remdesivir. Science (New York, N.Y.) 368, 1499–1504.

Zhao, J., Guo, S., Yi, D., Li, Q., Ma, L., Zhang, Y., Wang, J., Li, X., Guo, F., Lin, R., et al., 2021. A cell-based assay to discover inhibitors of SARS-CoV-2 RNA dependent RNA polymerase. Antivir. Res. 190, 105078.

Zhou, P., Yang, X.L., Wang, X.G., Hu, B., Zhang, L., Zhang, W., Si, H.R., Zhu, Y., Li, B., Huang, C.L., et al., 2020. A pneumonia outbreak associated with a new coronavirus of probable bat origin. Nature 579, 270–273.